

Contribution from Ames Laboratory—ERDA and the Department of Chemistry
Iowa State University, Ames, Iowa 50011

Metal–Metal Bonding in Reduced Scandium Halides. Synthesis and Characterization of Heptascandium Decachloride ($\text{Sc}_7\text{Cl}_{10}$). A Novel Metal-Chain Structure¹

KENNETH R. POEPPELMEIER and JOHN D. CORBETT*

Received January 3, 1977

AIC700087

The reaction of scandium metal with scandium trihalide in a sealed tantalum container under a temperature gradient 880–900 °C results in transport of monocrystals of heptascandium decachloride ($\text{ScCl}_{1.43}$) to the hot zone. The compound crystallizes in the monoclinic space group $C2/m$ with $a = 18.620$ (7) Å, $b = 3.5366$ (7) Å, $c = 12.250$ (5) Å, $\beta = 91.98$ (4)°, and $Z = 2$. Full-matrix least-squares refinement of all atoms with anisotropic thermal parameters gave final residuals $R = 0.059$ and $R_w = 0.072$ for 705 independent reflections with $2\theta \leq 50^\circ$ and $I > 3\sigma(I)$. The unique feature of the structure is the presence of infinite chains composed of two parallel chains of scandium octahedra which share a common edge. Chlorine atoms cap all outward facing metal triangles and also bridge (a) to and (b) between isolated Sc(III) metal ions, giving the connectivity description $(\text{ScCl}^b_{4/2}\text{Cl}^a_{2/3})_\infty(\text{Sc}_6\text{Cl}_6\text{Cl}^a_{4/3})_\infty$ where the fractional atoms Cl^a and Cl^b provide the bridging functions. The structure is thus intermediate between the single chains of octahedra found in $\text{GdCl}_{1.5}$ and the infinite two-dimensional sheets of edge-shared octahedra in ScCl . Magnetic susceptibility measurements between 79 and 297 K (Faraday method) indicate a Curie–Weiss behavior above ~ 120 K ($\mu = 1.04 \mu_B$, $\theta = -498$ K) with evidence of magnetic ordering at $T < 79$ K. This and a sharp EPR signal at room temperature ($g = 1.97$) are interpreted in terms of localized, weakly interacting (at 297 K) d^1 configurations for two (of six) particular scandium atoms in the chain. The occurrence of strongly bonded and well-separated metal chains and the physical properties resulting therefrom suggest the phase can be described as a crystalline analogue of a metal fiber composite.

Introduction

Heptascandium decachloride, $\text{Sc}_7\text{Cl}_{10}$, is the second in a plethora of reduced scandium chloride phases to be isolated and characterized. The checkered history and inherent problems with attaining equilibrium in the $\text{Sc}-\text{ScCl}_3$ system have been discussed in an earlier publication.² Briefly, a highly fibrous Sc_2Cl_3 ("mouse fur") can be obtained in small amounts when metal sheet is reacted at 700–800 °C with liquid or, better, gaseous ScCl_3 in sealed tantalum tubing.³ The combination of sesquichloride on metal exhibits a remarkable metastability up to the former's decomposition (melting) point of 877 °C in that their further reaction below this temperature over a period of several weeks is extremely limited and does not yield recognizable amounts of any intermediate phase. Notwithstanding, at least five phases can be recognized in x-ray powder diffraction patterns of products obtained from the same Sc_2Cl_3 -Sc reaction above this temperature, although the formation reactions are still very slow, presumably because of kinetic problems associated with the generation of extended metal–metal bonded networks. The problem of limited yield is reduced somewhat through the use of powdered Sc metal as the reductant in place of foil or turnings. The first phase identified in this study was ScCl , a double metal–double halogen sheet structure which is isostructural with ZrBr and closely related to ZrCl .^{2,4} The present paper reports the preparation, crystal structure, and magnetic and electron paramagnetic resonance properties of a second phase, $\text{Sc}_7\text{Cl}_{10}$.

Experimental Section

Synthesis. All preparations, manipulations, and analyses of materials were as previously described for ScCl .² The metal utilized had atomic impurity levels in ppm as follows: H, 585; C, 146; O, 266; F, 164; W, 20; Ta, 17; N, 13; Cu, 9; Fe, 50; individual rare earth elements and all others, <1. Powdered (<100 mesh) metal was again used as the reductant; for example, ca. 0.20 g of Sc and 0.59 g of ScCl_3 ($\text{Cl}:\text{Sc} = 1.4$ overall) were placed in a 4 cm long, 9-mm o.d. tantalum tube; this was welded and sealed in a fused silica jacket, and the contents heated in a gradient of 880–900 °C for 6 weeks. The crystals of interest here ($\text{ScCl}_{1.43}$) deposit as needles in the hottest reaches of the reaction container. Approximately 70% of the product by weight is found as a fibrous mass of very thin whiskers in the cold end of the reaction tube as another phase previously identified as $\text{Cl}:\text{Sc} = 1.45 \pm 0.03$ by chemical analysis. The whiskers resemble the

reported scandium sesquihalide phase³ in habit but they exhibit a quite different powder diffraction pattern and have a measurably different composition. The same $\text{ScCl}_{1.45}$ may also be obtained directly from $\text{ScCl}_{1.50}$ by reduction with metal foil between 877 and 885 °C. This material has the unusual property of undergoing an irreversible, erratic, and exothermic decomposition over the temperature range 885–895 °C according to thermal analysis. X-ray powder diffraction showed that $\text{Sc}_7\text{Cl}_{10}$ ($\text{ScCl}_{1.43}$) was the principal decomposition product on heating $\text{ScCl}_{1.45}$ at 900 °C for 30 min in sealed Ta tubing followed by air quenching. These observations led to the choice of the temperature gradient employed for single-crystal preparation.

Magnetic Susceptibility. Measurements were made on a Faraday apparatus constructed and calibrated in this laboratory.⁵ The null balance employed was a Cahn RG electrobalance with a sensitivity of 10^{-6} g. Approximately 100 mg of transported $\text{ScCl}_{1.43}$ was sealed under vacuum in a Pyrex ampule that had been cleaned in boiling aqua regia. Susceptibilities were determined between 77 and 297 K with the temperature monitored by a copper–constantan thermocouple bonded to the inner surface of the heater assembly and in the presence of 100 μ of He exchange gas to reduce temperature gradients between the heater and sample. The balance was zeroed with each temperature increment to allow for any possible convection currents. The Honda–Owen⁶ method for determination of field dependence was utilized; force measurements were made at five settings between 6 and 12 kOe at each temperature and $\chi(H = \infty)$ obtained by extrapolation. Then $\chi(H = \infty)$ was corrected for the temperature-dependent susceptibility of the Pyrex container, the data were converted to a molar basis, and finally diamagnetic core corrections were applied for Sc^{3+} and Cl^- (Selwood). Measurement of the room-temperature susceptibility before and after the low-temperature study demonstrated the absence of any hysteresis.

Electron Paramagnetic Resonance. The EPR spectrum was obtained at room temperature for a 10-mg polycrystalline sample from the same reaction product utilized for the magnetic susceptibility measurements and the structural determination. The spectrum was recorded on a Varian Model E-3 spectrometer with a frequency range of 8.8–9.6 GHz and a dial-selected magnetic field. The magnetic field was calibrated using strong pitch ($g = 2.0028$).

Crystal Selection. Relative to $\text{ScCl}_{1.50}$ or $\text{ScCl}_{1.45}$ the $\text{ScCl}_{1.43}$ crystals are still quite fibrous but have a marked increase in cross section. Considerable care must be taken not to fray them into whiskers by abuse or cutting. Suitable specimens were sealed in 0.3-mm i.d. Lindemann glass capillaries in a specially designed inert-atmosphere box constructed with a nearly horizontal window to facilitate the use of a stereozoom microscope. Preliminary zero-level Weissenberg photographs ($h0l$) revealed the crystals exhibited a range

Table I. Crystallographic Data

Composition: $\text{Sc}_7\text{Cl}_{10}$
 Cell: monoclinic, $C2/m$ (No. 12)
 Lattice parameters: $a = 18.620$ (7) Å, $b = 3.5366$ (6) Å, $c = 12.250$ (5) Å, $\beta = 91.98$ (4)°
 Refinement: $R = 0.059$, $R_w = 0.072$ (705 reflections, $2\theta \leq 49.9^\circ$)

ScI	Atom Positions						
	<i>x</i>	<i>y</i>	<i>z</i>	B_{11}^a	B_{22}	B_{33}	B_{13}
Sc1	0.0	0.0	0.0	1.25 (14)	1.67 (12)	1.26 (12)	0.27 (9)
Sc2	0.3314 (1)	0.0	0.2466 (2)	1.25 (14)	0.95 (8)	1.37 (7)	0.46 (9)
Sc3	0.1891 (1)	0.5	0.2935 (2)	1.39 (13)	1.08 (8)	1.44 (6)	0.36 (10)
Sc4	0.3164 (1)	0.5	0.4693 (1)	0.97 (14)	1.15 (9)	1.14 (6)	0.27 (9)
Cl1	0.4155 (1)	0.0	0.4042 (2)	1.39 (13)	1.40 (11)	1.62 (12)	0.36 (10)
Cl2	0.0988 (1)	0.0	0.3548 (2)	1.25 (14)	1.24 (11)	1.50 (12)	0.18 (9)
Cl3	0.0565 (1)	0.5	0.1192 (2)	2.08 (14)	1.27 (11)	1.98 (12)	0.27 (9)
Cl4	0.2150 (1)	0.0	0.1407 (2)	1.39 (13)	1.36 (8)	1.50 (12)	0.09 (9)
Cl5	0.3902 (1)	0.5	0.1208 (2)	2.35 (14)	1.20 (10)	2.58 (12)	1.55 (9)

^a $T = \exp[-1/4(B_{11}h^2a^{*2} + B_{22}k^2b^{*2} + B_{33}l^2c^{*2} + 2B_{12}hka^*b^* + 2B_{13}hla^*c + 2B_{23}klb^*c^*)]$. $B_{12} = B_{23} = 0$ by symmetry.

of imperfections in the a^*c^* network, ranging from those which produced two or three distinct diffraction maxima parallel to the film translation ([010]) through streaks to single diffraction maxima. Data were collected on two crystals over the period of this study with final parameters coming from one of the smaller crystals ($0.55 \times 0.06 \times 0.06$ mm) which exhibited discrete and sharp diffraction maxima. Contrasts between these results and those from a similar-sized crystal which gave broad but discrete peaks will be considered later. The fibrous character of the crystals and the striations on the long faces ($2\text{-}\mu$ period) which were clearly visible under high magnification ($150\times$) are both manifestations of the microscopic chain structure found.

The data crystal was mounted with the needle axis b nearly collinear with ϕ on a four-circle diffractometer designed and built in the Ames Laboratory,⁷ and four ω -oscillation photographs were taken at various ϕ settings. From these photographs 12 independent reflections were selected and their coordinates input into an automatic indexing program.⁸ The reduced cell and reduced-cell scalars which resulted indicated monoclinic symmetry and this was then confirmed by inspection of ω -oscillation photographs taken about each of the three reciprocal axes. Only the b axis showed the presence of a mirror plane and all three layer line spacings observed agreed with those predicted by the indexing routine.

Data Collection. X-ray data were collected at ambient temperature using Mo $K\alpha$ radiation ($\lambda 0.70954$ Å) monochromatized with a graphite single crystal. All reflections within a sphere defined by $2\theta \leq 50^\circ$ in the octants hkl and $h\bar{k}l$ were checked using an ω -scan mode. The peak heights of three standard reflections remeasured every 75 reflections to check on instrument and crystal stability did not show any change over the data collection period. Final cell parameters and their estimated standard deviations were obtained from the same data crystal by a least-squares refinement⁹ of $\pm 2\theta$ values of 19 independent reflections randomly distributed in reciprocal space ($2\theta > 25^\circ$) which were tuned by top-bottom, left-right beam splitting. The results were $a = 18.620$ (7) Å, $b = 3.5366$ (7) Å, $c = 12.250$ (5) Å, and $\beta = 91.98$ (4)°. The initial portion of the data set was collected on the basis of a primitive monoclinic cell but after measurement of a few hundred reflections the condition for C -centering, $h + k = 2n$, was obvious and this Bravais lattice type was imposed thereafter.

Structure Determination and Refinement. Programs for data reduction, structure solution, illustration, and sources of atomic scattering factors for neutral atoms (including corrections for both real and imaginary parts of anomalous dispersion) were as referenced before.^{4,10} The observed intensities were corrected for Lorentz-polarization effects and their standard deviations calculated as previously described¹¹ to yield 730 observed reflections ($I > 3\sigma(I)$) from a possible 877. Appropriate averaging of duplicate reflections yielded 705 independent data.

A preliminary structure determination of the $\text{ScCl}_{1.43}$ phase was first completed in the triclinic space group $P1$ utilizing a crystal which gave broad but discrete peaks and provided at best satisfactory diffraction data. Initial atomic positions were obtained by direct methods using MULTAN¹² and once the scandium and chlorine atoms were correctly differentiated three cycles of full-matrix least-squares refinement with isotropic thermal parameters converged at $R = \sum ||F_o|$

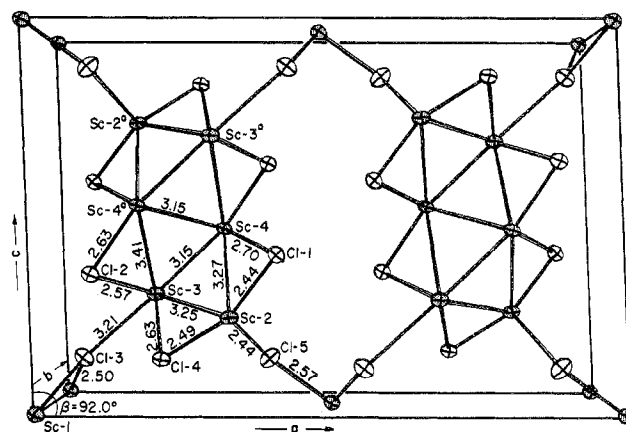


Figure 1. View of the $\text{Sc}_7\text{Cl}_{10}$ structure down the short b axis. Atoms Sc1, Sc2, Cl1, Cl2, and Cl4 are at $y = 0$; the remainder, at $y = 0.5$. Superscript atoms are related through the operation $1/2 - x, 1/2 - y, 1 - z$.

$-F_o|/\sum |F_o| = 0.146$. At this point a C -centered monoclinic cell appeared likely, the triclinic structure limiting the monoclinic space group to $C2/m$ with three scandium atoms and five chlorine atoms on special positions 4i and one scandium atom on special position 2a. Triclinic cell positions and data indices were then converted to the monoclinic basis for further refinement (see Discussion). Similar atom parameters were used as initial input for refinement with the better data set obtained from the crystal which gave sharper diffraction maxima. In this case three cycles of full-matrix least-squares refinement, varying the scale factor, positional parameters, and isotropic thermal parameters, converged at $R = 0.077$ and $R_w = 0.099$ where $R_w = [\sum w(|F_o| - |F_c|)^2 / \sum w|F_o|^2]^{1/2}$ and $w = \sigma_F^{-2}$. Further refinement with anisotropic parameters for all atoms gave convergence at $R = 0.059$ and $R_w = 0.072$. An absorption correction¹³ appropriate to the correct stoichiometry ($\mu = 43 \text{ cm}^{-1}$) and crystal shape was not considered necessary since transmission factors varied only from 0.813 to 0.834. At this point variation of all occupation parameters for both scandium and chlorine atoms gave converged values of 1.00 (1), indicating no significant deviation from the stoichiometry $\text{Sc}_7\text{Cl}_{10}$. A final difference Fourier synthesis map was flat to $\leq 1 \text{ e}/\text{Å}^3$ on atom sites and $\leq 0.5 \text{ e}/\text{Å}^3$ elsewhere.

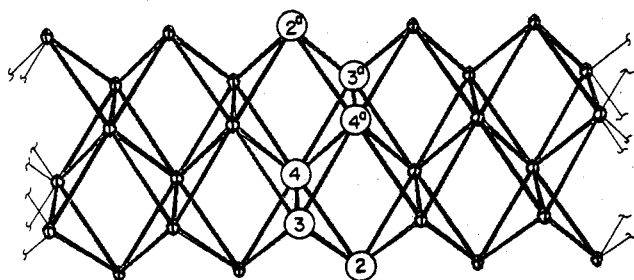
Results

Structure Description. Final positional and thermal parameters for $\text{Sc}_7\text{Cl}_{10}$ are listed in Table I, and important interatomic distances and angles are given in Table II. Structure factor results are available as supplementary material. Figure 1 is an ORTEP drawing of the structure viewed along the b axis which illustrates the spatial arrangement of all atoms in the unit cell. (Superscript letters refer to symmetry operations defined in Table II.) The occurrence of all

Table II. Bond Distances (Å) and Angles (deg) in $\text{Sc}_7\text{Cl}_{10}$

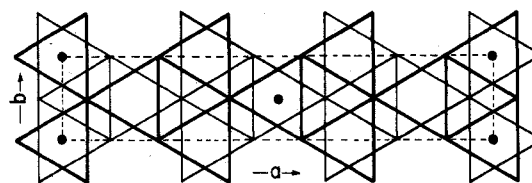
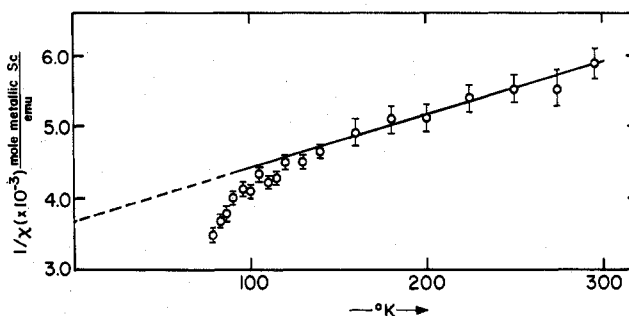
Metal Octahedra			
Distances			
Sc2-Sc3	3.253 (2)	Sc3-Sc4 ^a	3.407 (3)
Sc2-Sc4	3.271 (2)	Sc4-Sc4 ^a	3.153 (3)
Sc3-Sc4	3.147 (3)	Sc1-Sc1 ^d	3.5366 (6) (<i>b</i> axis)
Angles			
Sc4-Sc2-Sc3	57.69 (6)	Sc3-Sc4 ^a -Sc3 ^b	62.54 (5)
Sc3-Sc4-Sc2	60.87 (6)	Sc4 ^b -Sc4-Sc4 ^a	55.89 (4)
Sc2-Sc3-Sc4	61.43 (5)	Sc4-Sc4 ^a -Sc4 ^b	68.23 (8)
Sc3-Sc4-Sc4 ^a	65.46 (7)	Sc3-Sc3 ^b -Sc2	57.07 (3)
Sc4-Sc4 ^a -Sc3	56.19 (6)	Sc3-Sc2-Sc3 ^b	65.86 (5)
Sc4 ^a -Sc3-Sc4	57.36 (6)	Sc2-Sc4-Sc4 ^b	57.27 (3)
Sc4 ^a -Sc3-Sc3 ^b	58.73 (3)	Sc4-Sc2-Sc4 ^b	65.46 (6)
Chlorine Atoms on Metal Chain			
Distances			
Sc4-Cl1	2.695 (2)	Sc3-Cl2	2.570 (2)
Sc2-Cl1	2.443 (3)	Sc2-Cl4	2.487 (3)
Sc4 ^a -Cl2	2.627 (3)	Sc3-Cl4	2.631 (2)
Angles			
Sc4-Cl1-Sc4 ^b	82.02 (9)	Sc3-Cl2-Sc3 ^b	86.96 (9)
Sc4-Cl1-Sc2	78.91 (8)	Sc3-Cl4-Sc3 ^b	84.45 (9)
Sc4 ^a -Cl2-Sc3	81.91 (8)	Sc3-Cl4-Sc2	78.86 (9)
Bridging Chlorine Atoms			
Distances			
Sc3-Cl3	3.208 (4)	Sc2-Cl5	2.443 (3)
Sc1-Cl3	2.502 (2)	Sc1 ^c -Cl5	2.566 (3)
Angles			
Sc3-Cl3-Sc1	133.37 (5)	Sc2-Cl5-Sc1 ^c	134.36 (6)
Sc1-Cl3-Sc1 ^d	89.95 (9)	Sc2-Cl5-Sc2 ^d	85.28 (9)
Chlorine around Isolated Metal Atoms: Angles			
Cl5-Sc1 ^c -Cl3 ^c	90.54 (8)	Cl3-Sc1-Cl3 ^b	89.95 (9)

^a $1/2 - x, 1/2 - y, 1 - z$. ^b $x, y - 1, z$. ^c $1/2 + x, 1/2 + y, z$.
^d $x, y + 1, z$.

Figure 2. View of the metal-chain structure of $\text{Sc}_7\text{Cl}_{10}$ with the *b* axis horizontal. The distorted octahedra are discussed in the text in terms of those with apices 2-4^a and 4-2^a.

atoms at $y = 0$ or 0.5 along the $3.54\text{-}\text{\AA}$ *b* axis generates regular chains of scandium atoms in that direction, as shown in Figure 2. This remarkable consequence can be best constructed in two stages—first, infinite chains of distorted octahedra of scandium which share opposite edges Sc3-Sc4 and $\text{Sc3}^a\text{-Sc4}^a$ and, then, pairs of these chains displaced by $b/2$ and joined at a common edge, Sc4-Sc4^a . The octahedra are appreciably distorted; the waist of the octahedra as viewed in Figure 2 is a rectangle $3.15 \times 3.54\text{ \AA}$, and the apex Sc4^a is off-center with distances of 3.15 and 3.41 \AA to the waist atoms, a displacement which allows the formation of the short (3.15 \AA) $\text{Sc3}^a\text{-Sc4}^a$ bond in the other chain. The other apex Sc2 is relatively well centered above the waist rectangle at distances of $3.25\text{-}3.27\text{ \AA}$.

All chlorine atoms have three metal neighbors. Chlorine atoms 1, 2, and 4 cap all outward facing Sc triangles of the chain structure as illustrated in Figure 1 (e.g., $\text{Sc3-Sc3}^b\text{-Sc4}^a$) but do not cover those which are inward facing (e.g., Sc3-Sc4-Sc4^a) or those between apices of the octahedra (e.g.,

Figure 3. The [001] section of the $\text{Sc}_7\text{Cl}_{10}$ structure viewed down *c* showing close-packed layers generated by Cl3, -4, and -5 and (face-centered) octahedral interstices occupied by Sc1.Figure 4. Reciprocal molar (per mole of metallic scandium) magnetic susceptibility vs. temperature for polycrystalline $\text{Sc}_7\text{Cl}_{10}$.Table III. Susceptibility of Polycrystalline $\text{ScCl}_{1.43}$

Temp, K	$10^6\chi$, (sample), ^a emu/g	Temp, K	$10^6\chi$, (sample), ^a emu/g	Temp, K	$10^6\chi$, (sample), ^a emu/g
79	2.20 (4)	110	1.73 (3)	180	1.34 (4)
83	2.04 (1)	115	1.71 (4)	200	1.34 (3)
86	1.99 (2)	120	1.59 (1)	225	1.28 (3)
90	1.85 (1)	130	1.60 (4)	250	1.24 (4)
95	1.78 (4)	140	1.54 (2)	275	1.23 (7)
100	1.81 (1)	160	1.43 (5)	297	1.14 (4)
105	1.69 (1)				

^a The uncertainties in parentheses are standard deviations derived from the Honda-Owen plot.

$\text{Sc2-Sc2}^d\text{-Sc3}$) which would be too close to neighboring chlorine atoms (Cl4). Scandium-chlorine distances for this compound range from 2.44 to 2.70 \AA compared with 2.58 \AA in ScCl_3 ¹⁵ and 2.59 \AA in ScCl_2 ,² a similarity which again emphasizes the apparent disposition of the reduction electrons within the chains. Additional chlorine atoms 3 and 5 bridge between the metal chains and the isolated Sc1 atoms in a complementary fashion; that is, Cl3 edge-bridges two Sc1 atoms at a distance of 2.50 \AA and interacts with Sc3 through a long Sc-Cl bond, 3.21 \AA , whereas Cl5 bridges between two Sc2 apex atoms in the chains at 2.44 \AA and in addition is bonded to Sc1 at 2.57 \AA (as shown at $1/2, 1/2, 0$).

Another structural regularity is found in the two close-packed chlorine layers generated about (001) by chlorine atoms 3, 4, and 5, where the isolated Sc1 (presumably scandium(III)) atoms occupy one-third of the octahedral interstices, as shown in Figure 3. The octahedra containing these isolated metal atoms also form chains parallel to the *b* axis.

Magnetic and EPR Data. The gram-susceptibility of $\text{ScCl}_{1.43}$ (χ_g) as a function of temperature is provided in Table III, and Figure 4 is a plot of $(\chi_M^* - \chi_D)^{-1}$ vs temperature where χ_M^* is the molar paramagnetism assigned to the metallic scandium, that is, chain metal atoms Sc2, Sc3, and Sc4 but not the unique Sc1.¹⁶ The compound exhibits Curie-Weiss behavior above about 120 K , and the data yield values of $1.04\text{ }\mu_B$ and -498 K for μ_{eff} and Θ , respectively, when calculated per mole of metallic scandium. Although the low-temperature magnetic behavior is not yet known, the data shown suggest the compound may order antiferromagnetically with T_N somewhat below 79 K . Figure 5 is a reproduction

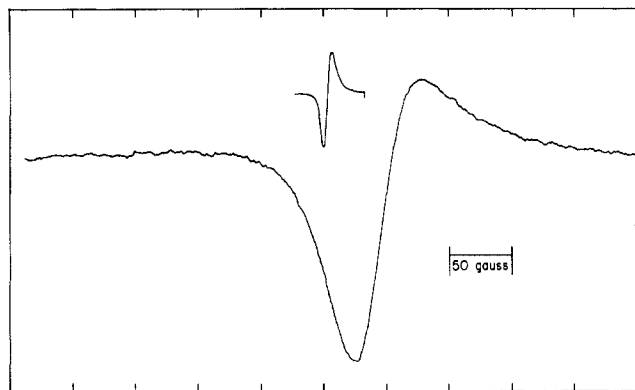


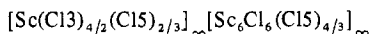
Figure 5. EPR spectrum of polycrystalline $\text{Sc}_7\text{Cl}_{10}$ at room temperature.

of the EPR spectrum of $\text{ScCl}_{1.43}$ at room temperature from which the g factor is calculated to be 1.97.

Discussion

The $\text{Sc}_7\text{Cl}_{10}$ structure represents an intermediate degree of metal-metal bonding relative to two other very reduced ($\text{Cl}:\text{M} < 2.0$) rare earth metal chlorides, $\text{GdCl}_{1.5}$ ¹⁷ and ScCl .² The gadolinium compound contains infinite chains of elongated octahedra which are clearly conceptual precursors of the double chains of metal octahedra found here and which also show the same type of face capping by chloride. Alternatively the double chain of octahedra can be generated by extracting a section through the ScCl structure, the original $\text{Cl}-\text{Sc}-\text{Sc}-\text{Cl}$ layers running vertically and normal to the paper in the section shown in Figure 1. The present structure retains the same capping halogen atoms 1 and 2 and "stitches up" the edges of the chains with Cl_4 and Cl_5 .

A useful description of the present structure can be obtained in terms of atom connectivity, an approach which has found considerable utility with discrete clusters.¹⁸ If the long $\text{Sc}-\text{Cl}_3$ interaction (3.21 Å) is considered unimportant, the structure sorts out as



where the first portion contains the isolated Sc_1 atom and associated bridging chlorines, the subscripts denoting the degree of sharing, and the second pair of brackets includes the integral repeating parts of the metal-bonded chain with capping and bridging (Cl_5) atoms. The isolated Sc_1 atom must be taken as a scandium(III) judging from distances to neighboring chlorine atoms since an added electron should markedly increase the effective radius. Thus there is an obvious element of electron transfer from Sc_1 to the metal chain and some chlorine transfer as well is implied by the above formulation.

A striking feature of this remarkable structure is the short metal-metal bonds; the shared edges between the octahedra in each chain (Sc_3-Sc_4), and between chains ($\text{Sc}_4-\text{Sc}_4^a$) at 3.147 (3) and 3.153 (3) Å, respectively, are the shortest scandium metal-metal distances known, considerably less than the shortest metal-metal distance in ScCl_2 , 3.216 (6) Å, and in the metal itself, 3.26 Å.¹⁹ The short distances correspond to a Pauling¹⁹ bond order of about 0.6, to the extent that this calculation is meaningful for such an asymmetric environment.

Undoubtedly the one-dimensional strongly bound metal-metal chains in $\text{Sc}_7\text{Cl}_{10}$ constitute the backbone of the structure, with only van der Waals interactions between parallel chains save for the indirect chlorine bridging between chains provided principally by Cl_5 via the isolated Sc_1 atoms. The fibrous crystal habit and the parallel striations observed on the crystal surfaces also attest to the highly anisotropic

bonding. An interesting measure of these effects is the difference in structural parameters obtained with diffraction data from two crystals of evidently different degrees of perfection utilizing the same instrument and techniques. The widths of "sharp" diffraction peaks out the axes of the final data crystal (e.g., (400), (080), (004)) were 0.06–0.10° at half-height, while these same diffraction maxima were 2.4–4 times broader with the less perfect crystal studied first. Likewise the refined structure deduced from the first crystal was satisfactory but not great ($R = 0.101$ for 642 reflections), the standard deviations of the parameters being 1.5–3 times those reported here. More remarkable is the consistent shift to shorter as well as more precisely determined interatomic distances and cell length in the better refined and "tighter" crystal. Unit cell dimensions in the latter were consistently smaller, 0.19 (5), 0.17 (2), 0.19 (5)%, respectively, leading to a remarkable 0.5% reduction in the cell volume, 810.48 (26) to 806.22 (51) Å³ or a difference of 7σ ! Presumably the increased degree of perfection occurs particularly in the packing or order of one scandium chain relative to the other along crystal defects. Although most thermal parameters were simply better defined with the better crystal data and not significantly different, the values of B_{11} for all chain atoms uniformly decreased by 9–10 σ . Although the bridging atoms Cl_3 , Cl_5 , and Sc_1 are crystallographically unique and perhaps less tightly bound, the relatively large values for B_{11} and B_{33} for Cl_5 (and Cl_3 to a smaller degree) and for B_{22} for the isolated Sc_1 (Table I) may or may not reflect remnant crystal defects.

The magnetic and EPR data for $\text{ScCl}_{1.43}$ are particularly helpful in assessing something of the electron distribution in the metal-metal bonded chains. The magnetic behavior also contrasts with that of either the two-dimensional metallic halides ThI_2 and LaI_2 ^{20,21} which exhibit only temperature-independent Pauli paramagnetism or the one-dimensional $\text{GdCl}_{1.5}$ where the dominant $4f^7$ cores obscure any possible details regarding the bonding.²² However the $\text{ScCl}_{1.43}$ data show a considerable parallel with the magnetic behavior of scandium metal²³ where a Curie-Weiss behavior with $\mu_{\text{eff}} = 1.65 \mu_B$ and $\Theta = -850$ K compares with $1.04 \mu_B$ and -498 K here. If the one-dimensional character of the scandium metal chains of octahedra in $\text{ScCl}_{1.43}$ and the reduction in the number of free valence electrons per metal atom corresponding to partial oxidation are considered, the smaller magnitude of both the magnetic moment and Weiss constant found here seem reasonable and plausible. For this low-dimensional and anisotropic compound an interpretation of the results in terms of partially localized spin states is at least instructive if not necessary.²⁴ Symmetry does not restrict all metal atoms to magnetic equivalence in $\text{ScCl}_{1.43}$; in fact consideration of the differences in bond length, coordination, etc., between metal atoms Sc_2 , $-\text{Sc}_3$, $-\text{Sc}_4$ and Sc_2^a , $-\text{Sc}_3^a$, $-\text{Sc}_4^a$ leads to the opposite assumption. The effective magnetic moment calculated for the molar composition $\text{Sc}_7\text{Cl}_{10}$ is $2.57 \mu_B$, a value close to the spin-only value for two unpaired electrons. Although these could be localized on any pair or, in part, pairs of metal atoms in the $\text{Sc}_7\text{Cl}_{10}$ repeating unit, the symmetry uniqueness of the Sc_2 apical sites and their longer bond distances to waist sites are consistent with unpaired electrons localized on these sites (Sc_2 and Sc_2^a). The room-temperature EPR spectrum clearly supports the presence of localized and relative weakly coupled electrons (50-G line width), as should be the case for these Sc_2 sites. With an experimental g factor of 1.97 the calculated $\mu_{\text{eff}} = 2^{1/2}(1.97)[1/2(1/2 + 1)]^{1/2} = 2.41$ is in good agreement with that determined from the magnetic susceptibility (2.57).

The plethora of reduced phases known to exist in the $\text{Sc}-\text{ScCl}_3$ system² will undoubtedly reveal phenomenologically the more or less continuous process of metal catenation and electron delocalization as a function of metal content and

oxidation state. A phase is presently under investigation which clearly contains discrete six-atom metal clusters²⁵ (bond distances 3.21–3.23 Å), thus representing the end member of the metal–metal bonded series extending from isolated octahedral metal clusters through chains to two-dimensional sheets of shared metal octahedra. In addition the phase $\text{ScI}_{2.15}$ in a CdI_2 -type structure evidently exhibits a metallic conduction for only single sheets of metal atoms.²⁶ Seldom has one element provided such a versatile and exciting opportunity to view metal–metal bonding and the properties derived thereby over such a range of structural complexity and, presumably, electron delocalization.

The didactic concept of cluster condensation recently put forth by Simon^{27,28} to account for structural similarities in metal-rich compounds works quite well to describe the chains of shared but distorted octahedra in $\text{Sc}_7\text{Cl}_{10}$. However, the presence of isolated $\text{Sc}(\text{III})$ ions is not predicted or accounted for by this type of modeling. This new variation reveals another important dimension in the structure of metal-rich phases, one that emphasizes the need for electronic models to complement a geometric scheme of cluster condensation. Obviously the radial extension of 3d orbitals early in the series is favorable for metal–metal bonding, contrary to some expectations, but the richness and diversity of this feature with scandium requires further definition of more subtle factors than just the commonly accepted^{29,30} orbital size.

Acknowledgment. The authors thank Dr. R. A. Jacobson for assistance and use of the diffractometer and many helpful suggestions concerning the refinement, J. D. Greiner for his help with the determination of the magnetic susceptibility, Dr. B. Harmon for his comments on alternative interpretations of these data, and Dr. R. McGinnis for running the EPR spectrum.

Registry No. $\text{Sc}_7\text{Cl}_{10}$, 61966-52-7.

Supplementary Material Available: Listing of observed and calculated structure factor amplitudes (3 pages). Ordering information is given on any current masthead page.

References and Notes

- (1) Work performed for the U.S. Energy Research and Development Administration under Contract No. W-7405-eng-82.
- (2) K. R. Poeppelmeier and J. D. Corbett, *Inorg. Chem.*, **16**, 294 (1977).
- (3) B. C. McCollum, M. J. Camp, and J. D. Corbett, *Inorg. Chem.*, **12**, 778 (1973).
- (4) D. G. Adolphson and J. D. Corbett, *Inorg. Chem.*, **15**, 1820 (1976).
- (5) J. G. Converse and R. E. McCarley, *Inorg. Chem.*, **9**, 1361 (1970).
- (6) L. F. Bates, "Modern Magnetism", 3d ed, Cambridge University Press, Cambridge, England, 1951, pp 133–136.
- (7) W. J. Rohrbach and R. A. Jacobson, *Inorg. Chem.*, **13**, 2535 (1974).
- (8) R. A. Jacobson, "An Algorithm for Automatic Indexing and Bravais Lattice Selection. The Programs BLIND and ALICE", U.S. Atomic Energy Commission Report IS-3469, Iowa State University, Ames, Iowa, 1974.
- (9) F. Takusagawa, personal communication, Ames Laboratory, 1975.
- (10) D. G. Adolphson, J. D. Corbett, and D. J. Merryman, *J. Am. Chem. Soc.*, **98**, 7234 (1976).
- (11) S. L. Lawton and R. A. Jacobson, *Inorg. Chem.*, **7**, 2124 (1968).
- (12) P. Main, M. M. Woolfson, and F. Germain, "MULTAN, a Computer Program for the Automatic Solution of Crystal Structures", University of York Printing Unit, York, U.K., 1971.
- (13) J. D. Scott, Queen's University, Kingston, Ontario, private communication, 1971.
- (14) "International Tables for X-Ray Crystallography", Vol. III, 2nd ed, Kynoch Press, Birmingham, England, 1962.
- (15) W. Klemm and E. Krose, *Z. Anorg. Allg. Chem.*, **253**, 218 (1947).
- (16) $\chi_M^* = \chi_g M^2/6$ where M is the formula weight of $\text{ScCl}_{1.43}$, and the factor $7/6$ accounts for the difference in types of metal atoms.
- (17) D. A. Lokken and J. D. Corbett, *Inorg. Chem.*, **12**, 556 (1973).
- (18) H. Schäfer and H. G. Schnering, *Angew. Chem.*, **76**, 833 (1964).
- (19) L. Pauling, "The Nature of the Chemical Bond", 3rd ed, Cornell University Press, Ithaca, N.Y., 1960, pp 400, 410.
- (20) R. J. Clark and J. D. Corbett, *Inorg. Chem.*, **2**, 460 (1963).
- (21) J. D. Corbett, R. A. Sallach, and D. A. Lokken, *Adv. Chem. Ser.*, No. 71, 56 (1967).
- (22) J. D. Greiner, J. F. Smith, J. D. Corbett, and F. J. Jelinek, *J. Inorg. Nucl. Chem.*, **28**, 971 (1966).
- (23) F. H. Spedding and J. J. Croat, *J. Chem. Phys.*, **58**, 5514 (1973).
- (24) The temperature dependence of the magnetic susceptibility of Sc was originally interpreted²⁵ in terms of a single localized 3d electron. However the polarized neutron diffraction behavior of scandium in an applied magnetic field is not consistent with this interpretation: W. C. Koehler and R. M. Moon, *Phys. Rev. Lett.*, **36**, 616 (1976).
- (25) K. R. Poeppelmeier and J. D. Corbett, to be submitted for publication.
- (26) B. C. McCollum and J. D. Corbett, *Chem. Commun.*, 1666 (1968).
- (27) A. Simon, *Chem. Unserer Zeit*, **10**, 1 (1976).
- (28) A. Simon, H. Mattausch, and H. Holzer, *Angew. Chem., Int. Ed. Engl.*, **15**, 624 (1976).
- (29) J. C. Sheldon, *Aust. J. Chem.*, **17**, 1191 (1964).
- (30) J. E. Ferguson, *Prep. Inorg. React.*, **7**, 93 (1971).

Contribution from the Department of Chemistry,
The University, St. Andrews, Scotland

Proton Magnetic Resonance Spectra of $\text{Lu}(\text{acac})_3 \cdot 2\text{H}_2\text{O}$ in Solution

JAMES A. KEMLO, J. DUNCAN NEILSON, and T. MAURICE SHEPHERD*

Received November 6, 1976

AIC60809U

^1H NMR spectra of $\text{Lu}(\text{acac})_3 \cdot 2\text{H}_2\text{O}$ in several solvents are reported, where $\text{acac} = \text{CH}_3\text{COCHCOCH}_3^-$. The spectral profiles are temperature dependent in benzene and toluene solutions and the multiplicity of ligand methyl resonances is attributed to slow exchange between nonequivalent methyl groups in a dimeric structure. The temperature dependence in acetone solution is consistent with the presence of a monomer–dimer equilibrium with $\Delta H^\circ = -28.2 \pm 1.5 \text{ kJ mol}^{-1}$ and $\Delta S^\circ = -74.5 \pm 4.5 \text{ J K}^{-1} \text{ mol}^{-1}$. The single ligand methyl and 3-H resonances in the strongly coordinating solvents dimethyl sulfoxide and pyridine indicate the sole presence of solvated monomers. Previous proposals about the anomalous spectrum of $\text{Mg}(\text{acac})_2$ in CDCl_3 are also discussed.

Recent investigations^{1,2} of intermolecular energy transfer between the metal ions of lanthanide acetylacetonates in solution have shown that the transfer process is solvent dependent. Three main types of behavior have been observed and have been rationalized in terms of the possible solution species occurring in the various solvents. It has been proposed that (a) in nonpolar solvents, e.g., benzene, kinetically stable dimers are present, (b) in polar but not strongly coordinating solvents, e.g., acetone, a monomer–dimer equilibrium exists

with a relatively rapid exchange rate, and (c) in strongly coordinating solvents, e.g., dimethyl sulfoxide, only solvated monomeric species are present. In order to obtain further information regarding the nature of the complex species in solution we have investigated the ^1H NMR spectra of the diamagnetic lutetium acetylacetonate complex, $\text{Lu}(\text{acac})_3 \cdot 2\text{H}_2\text{O}$, in these solvents and report the results below. The possible implications of these results with respect to a previous interpretation³ of the anomalous NMR spectrum of $\text{Mg}(\text{acac})_2$